Research Journal of Applied Sciences, Engineering and Technology 6(14): 2550-2560, 2013
DOI:10.19026/rjaset.6.3737
ISSN: 2040-7459; e-ISSN: 2040-7467

Submitted: December 26, 2012 Accepted: February 08, 2013 Published: August 10, 2013

Research Article

Computational Fluid Dynamics Simulation and Experimental Validation of Hypersonic Turbulence Boundary Layer

Xiao Hong, Shang Yuhe, Wu Di and Gao Xiaocheng
School of Power and Energy, Northwestern Polytechnical University, Xi'an 710072, China

Abstract: Numerical simulation and experimental validation of a hypersonic flat plate and isothermal turning wall flow were conducted in the current study. The investigation was based on three kinds of grids (Grid1, Grid2 and Grid3) with laminar flow and three types of turbulence models (BL, SA and SST). Under the same initiation and different turbulence models, the convergence process of the friction drag coefficient C_P and the Stanton number *St* of a hypersonic flat plate flow revealed four results. First, the flow turbulence effect in the BL model simulation was responsive to C_P and *St*. Second, the SA and SST model simulations both reflected the development process of flow turbulence. Third, the flow turbulence effect in the SST model simulation did not gradually emerge until the laminar flow simulation was sufficient. Moreover, the SA model simulation did not exist on such obvious hysteresis. Fourth, by comparing C_P and *St* of a hypersonic flat-plate laminar simulation under the three grids, the errors of the calculation results of Grid2 and Grid3 were small. In contrast, the error on Grid1 was large. By comparing C_P and *St* of the BL model for the three grids, we found that the result of Grid3 was slightly better than the result of Grid2. The deviation between them basically remained within 10%. However, the result of Grid1 had a large deviation with oscillation. C_P and *St* of the SA model for the three grids were then compared. A large difference was found only on the transition zone location between the result of Grid2 and Grid3. Nevertheless, the error and calculation of reference between them was maintained within 10%. Grid1 not only had a large deviation, but also had certain oscillation on the laminar flow area. Finally, C_P and *St* of the SST model for the three grids were compared. There was a large difference only on the transition zone location between the result of Grid2 and Grid3, but the error between them was maintained within 10%. Grid1 had a large deviation. The hypersonic flat-plate laminar flow was also compared with C_P and *St* calculated from the three turbulence models for the three grids. Evidently, the grids near the wall must be encrypted to an appropriate extent to simulate more accurately the boundary laminar flow as well as obtain proper surface friction and heat flow. The calculation in the present study showed that the Reynolds number in the first layer of the grid was more reasonable when it was about 20. The simulation result for the hypersonic isothermal two-dimensional turning wall flow showed that the calculation and experiment results from the different turbulence model were consistent. There was little difference between the location of the simulated heat flow peak and the position given by experiment. However, the peak, the curve trend after the peak and the experimental result widely differed. The curve and experimental results for pressure distribution greatly varied because of the existence of an isolated area in the calculation of the laminar flow. The calculation and experimental results from different turbulence models were close. The curve trend, the peak and the experimental result basically matched.

Keywords: Grid, hypersonic, BL, SA, SST, turbulence model

INTRODUCTION

With the development of the hypersonic vehicle, the complexity of the flow field is obviously improved. The most prominent feature is the existence of significant aerodynamic heating phenomena on the surface of a hypersonic vehicle. Therefore, the design requirement of thermal protection for a hypersonic vehicle is greatly increased. Previous differences between calculation and experimental results have shown that the assumption of laminar flow using the whole flow field could not accurately predict surface heat flow and local friction. A reasonable pressure distribution could not even be provided (Holden, 2000). Therefore, to simulate accurately a complex hypersonic flow field researchers have committed to improving the quality of grid generation and using a high-precision difference scheme. These processes enhance the resolution of numerical simulations (Jean *et al.*, 1998). Other researchers have abandoned the original assumption of laminar flow. They have taken the turbulence flow effect into account within the boundary layer or the entire flow field. Related items reflecting the turbulence flow effect in fluid equations have also been introduced (Yamamoto, 2001).

Corresponding Author: Xiao Hong, School of Power and Energy, Northwestern Polytechnical University, Xi'an 710072, China

To study the effect of a hypersonic flow numerical stimulation caused by grid and turbulence models, the present study numerically simulates a hypersonic flat plate and an isothermal two-dimensional turning wall flow. The simulation results are compared with the experimental results.

MATERIALS AND METHODS

Flow simulation of flat plate: The current study mainly aimed to assess the accuracy of two important flow field parameters. These parameters were the friction drag coefficient C_P and the Stanton number *St* of three types of turbulence model simulations including BL, SA and SST. The transition characteristics of different turbulence models were determined with a numerical study according to experimental results (Arthur, 2001). The purpose was to simulate accurately the transition area from the laminar to turbulence flows, especially the distribution of C_P and *St* at the end of the transition area. The transition locations were as follow:

Experimental result : (0.122 m, 0.264 m)
BL model : (0.122 m, 0.264 m)
SA model : (0.122 m, 0.188 m)
SST model : (0.071 m, 0.264 m)

Condition and method of calculation: The flow parameters were as follow:

$M_\infty = 6.0$, $T_\infty = 65.04K$, $T_w = 106.67K$ and $R_{e\infty} = 2.638 \times 10^7(1/m)$

The calculation method involved using AUSMPW+ flux as the splitting method, min_3U as the interpolation limiter, discrete grid as the five-point template, original variable NND as the implicit scheme, Reynolds-average NS equation as the governing equation, finite volume as the discretization method and LU decomposition technique as the discrete equation.

Computational grid: The boundary layer is usually very thin and the normal gradient of flow field parameter is very large. Therefore to simulate accurately the structure of the flow field in this part, the distribution of the grid structure and point of the flow field must be paid sufficient attention. Usually, the characterization of the grid resolution within the boundary layer needs the two indicators. The distance from the first layer of the grid to the body surface and the minimum grid points are also normally required. y^+_1 is used to measure the distance y_1 from the first layer of the grid to the body surface. Hence, the limit of y^+ needs to be converted to the limit of y when constructing the real grid:

$$y_1 = \frac{\nu}{u_\tau} y_1^+ = \sqrt{\frac{2}{C_f}} \frac{\nu}{V_\infty} y_1^+ = \sqrt{80} R_{ex}^{1/14} \frac{L}{R_{eL}} y_1^+ \quad (1)$$

Table 1: Values of Δy_1 for three grid types

Grid	Normal direction×flow direction）	Δy_1(m)
Grid1	161 × 191	9.652e-6
Grid2	161 × 191	9.652e-7
Grid3	161 × 191	9.652e-8

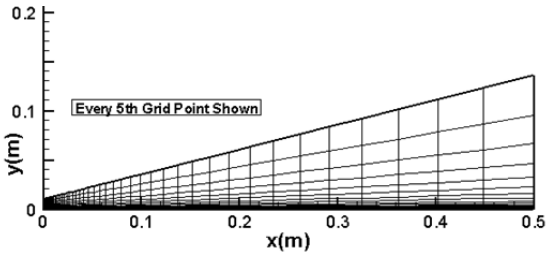

Fig. 1: Computing grid diagram of flat plate

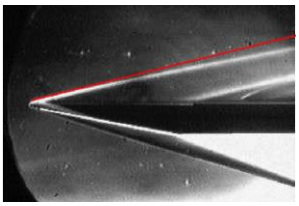

Fig. 2: Schlieren photo (M =8) (Purtell, 1992) of flat plate

In the above equation, $R_{ex} = V_\infty x/v$ is the local Reynolds number $R_{eL} = V_\infty L/v$, x is the flow distance from the calculation to stagnation points, L is the flow length of the aircraft and C_f is the local friction coefficient. C_f here uses the experimental result of an in compressive flat plate (Gao, 2005).

$$C_f = 2\left(\frac{u_\tau}{V_\infty}\right)^2 = 0.025 R_{ex}^{-1/7} \quad (2)$$

Once the upper limit of y^+_1 is given, the upper limit of y_1 can be approximated. On the three turbulence models studied in the present study, the demand of the SST model was the highest and the BL model was the lowest for y^+_1. Hence, the upper limit $y^+_{max} = 0.2$ of the SST model y^+_1 was used for convenient comparison.

Usually, a reasonable encryption of a grid can accurately simulate the flow field and improve the calculation reliability. However, excessive encryption is likely to cause numerical rigidity. For this problem, the accuracy of the calculation was compared with the effect of the calculation speed for all models caused by the spacing size in the first grid layer. Using the three computational grids, the specific parameters were determined, as shown in Table 1.

Calculation results and analyses: Figure 1 and 2 shows the experimental schlieren photograph. Figure 3

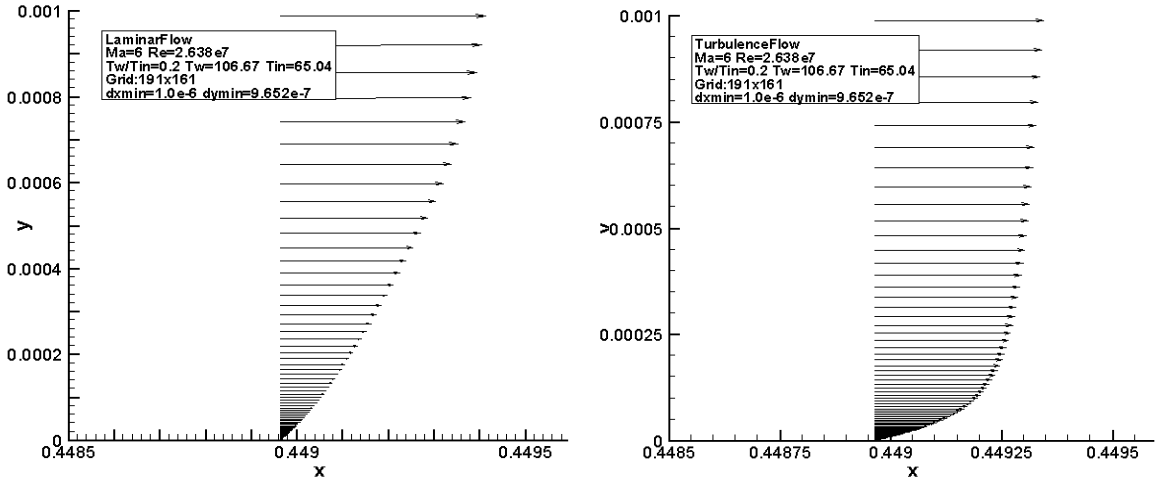

(a) (b)

Fig. 3: Velocity vector of boundary layer ; (a) : Laminar flow; (b): Turbulence flow

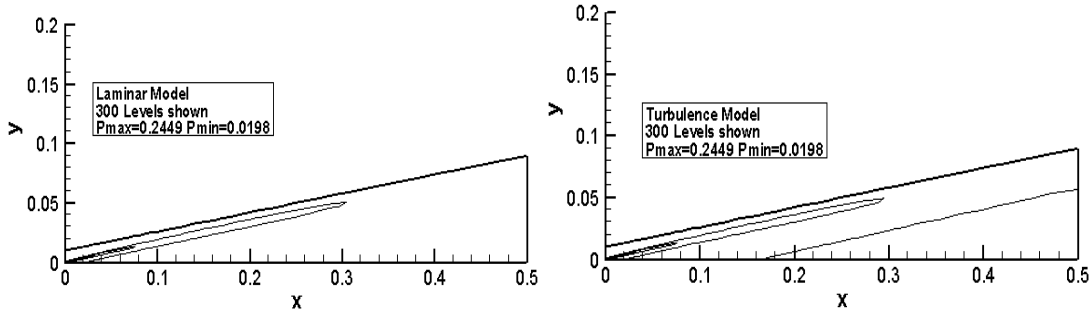

(a) (b)

Fig. 4: Pressure contours ; (a) : Laminar flow; (b) : Turbulence flow

shows the enlarged velocity vector map near the boundary layer of the same flow location when simulating laminar flow and turbulence. Clearly, the velocity distribution of turbulence was fuller than the laminar flow. This finding is consistent with the basic fact that the turbulence boundary layer is thicker than the laminar flow boundary layer. The difference between the two boundary layers is about two-fold.

Figure 4 shows the pressure contours of the flow field for the simulation of laminar flow and turbulence. The contours were equally divided and the two figures were compared. The results showed that prior to the transit of the flat plate, the pressure distribution between them had no significant difference. In the transition area, a compression wave appeared because of the rapid thickening of the boundary layer flow field of turbulence. This result was consistent with the experimental result of Fig. 2.

Figure 5 shows the wall pressure distribution of the different model calculations. The result of the laminar flow simulation was 5% smaller than those of the three turbulence models. However, the difference between

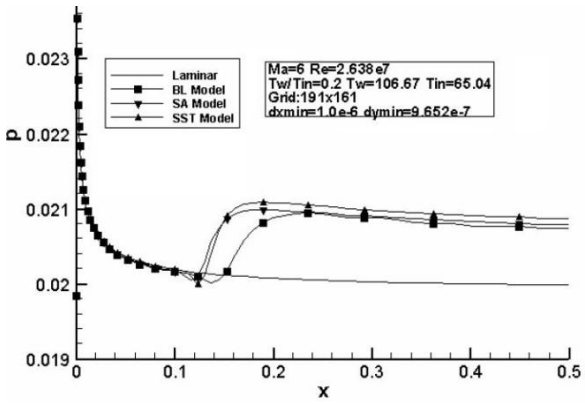

Fig. 5: Pressure distribution curve of wall

the turbulence models was up to 0.6%. The three turbulence models all captured the compression process of flow in the transition area from the laminar to turbulence flows.

Figure 6 shows the contrast between the calculation and experimental results (Purtell, 1992) of the Stanton

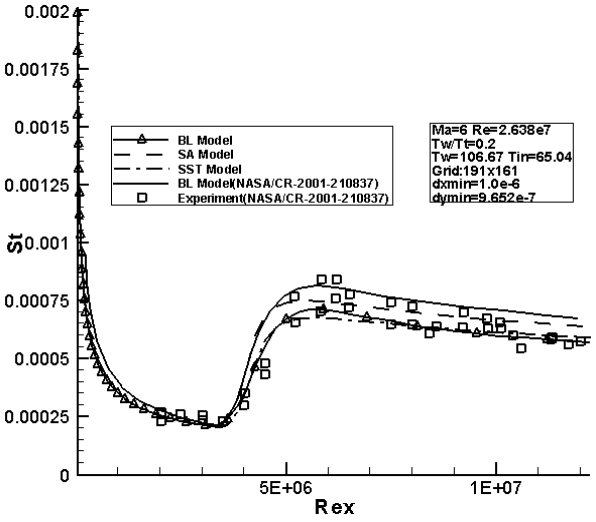

Fig. 6: The contrast of calculation and reference data of Stanton number for wall

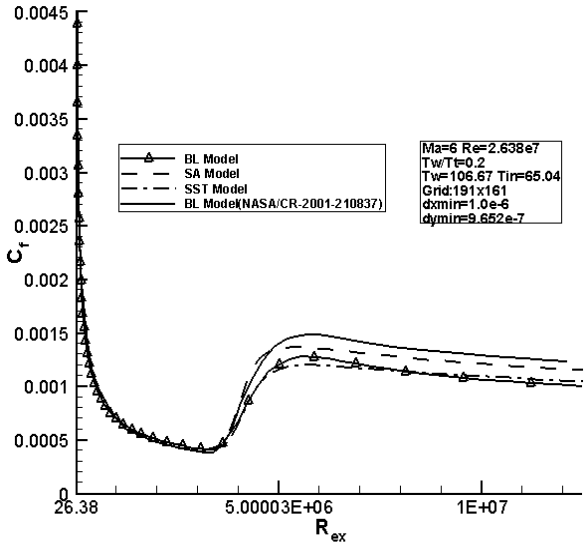

Fig. 7: The contrast of calculation and reference data of friction coefficient for wall

number for the different computing models. The calculation, experimental and reference results for the three turbulence models were all very close, but the simulations of the Stanton number peak were all low. Meanwhile, the curve trend between the calculation and experimental results had a certain difference that was acceptable according to the spreading law of the experimental result.

Figure 7 shows the contrast between the calculation and reference results (Purtell, 1992) of local friction for the different computing models. The calculations of the three turbulence models were all lower than the calculation of reference. The simulation in the transition area also had a certain difference. Different transition methods had different effects. The calculations of the BL and SST models were very close. These results indicated that the accuracy of the BL model was not lower than the accuracy of the SST model in a simple flow simulation.

Figure 8-11 show the convergence process of friction and the Stanton number for the different models under the same condition. The turbulence effect of the BL model immediately reflected heat flow and friction. However, the SA and SST models both reflected the development process of turbulence. The turbulence effect of the SST model slowly emerged only when the simulation of the laminar flow was sufficient. Nevertheless, there was no such obvious hysteresis on the SA model. The initial flow had different impacts on the convergence rates of the different turbulence models.

Figure 12 shows the contrast between friction and the Stanton number of the laminar flow simulation for the three grids. There was a small difference between the calculations of Grid2 and Grid3. On the other hand, the difference of Grid1 was up to several times, which was not believable.

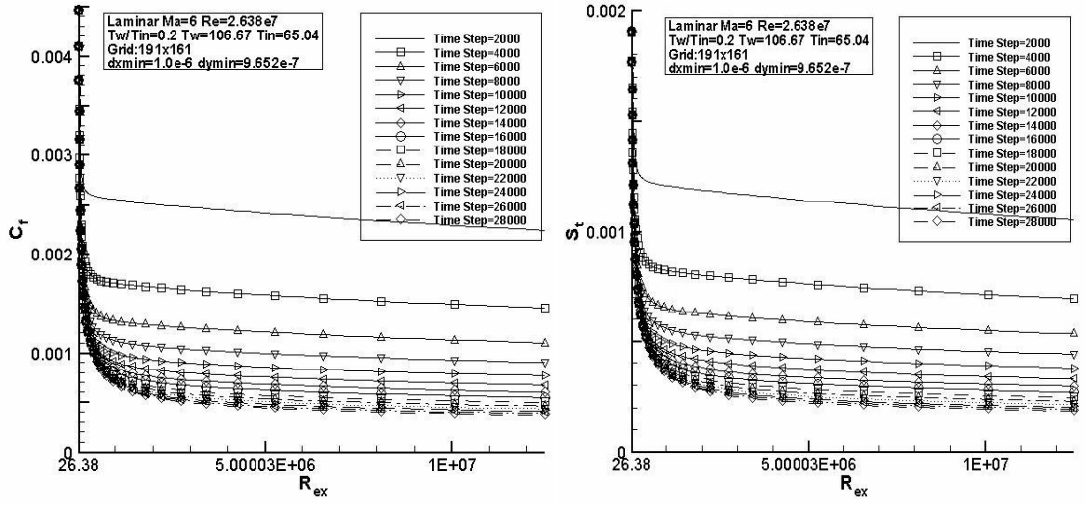

Fig. 8: Convergence process of wall friction coefficient and Stanton number for simulation of laminar flow

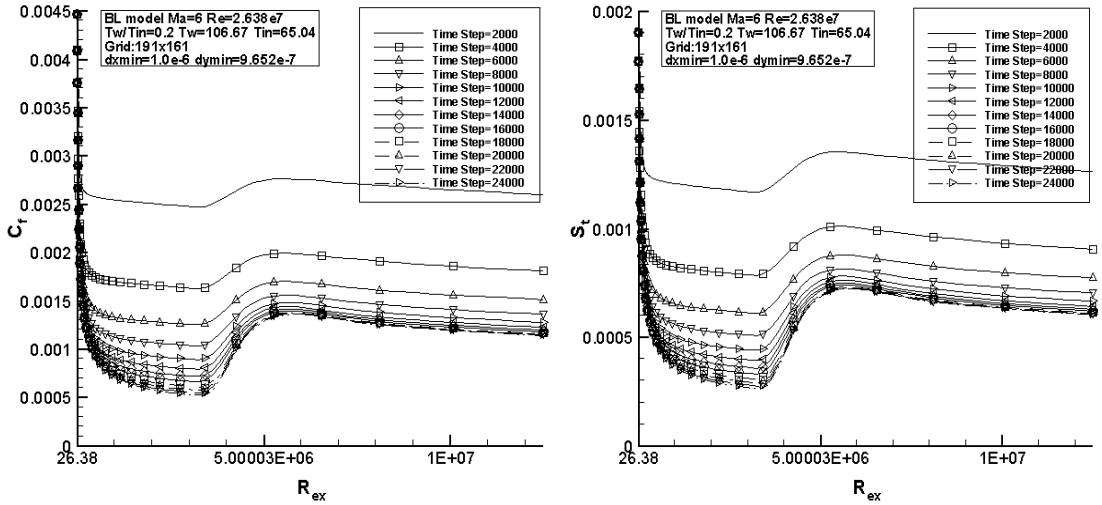

Fig. 9: Convergence process of wall friction coefficient and Stanton number for simulation of BL model

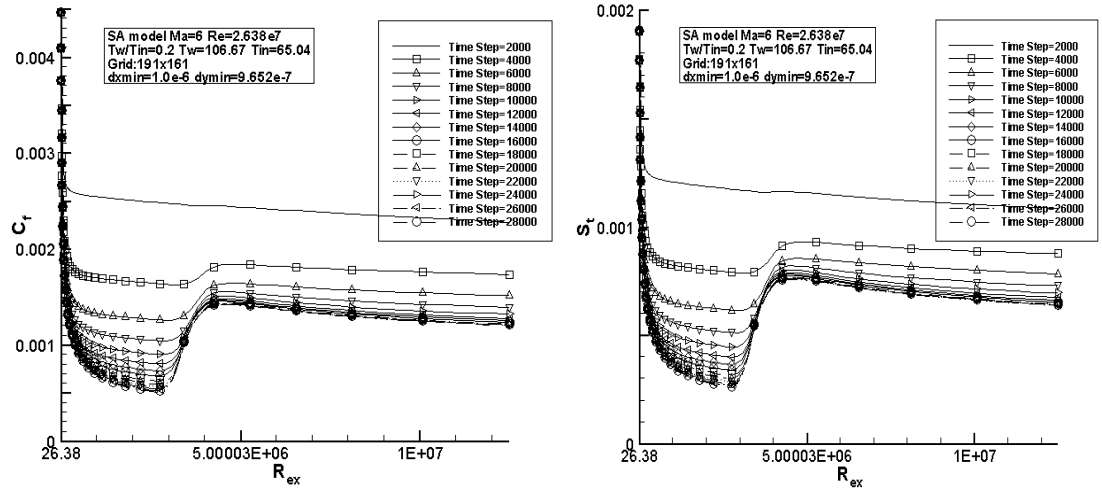

Fig. 10: Convergence process of wall friction coefficient and Stanton number for simulation of SA model

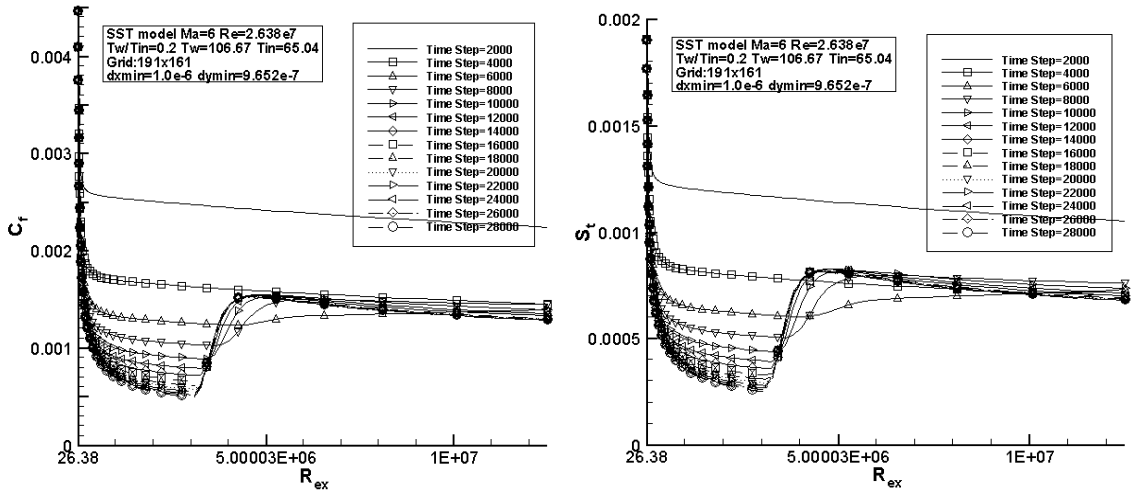

Fig. 11: Convergence process of wall friction coefficient and Stanton number for simulation of SST model

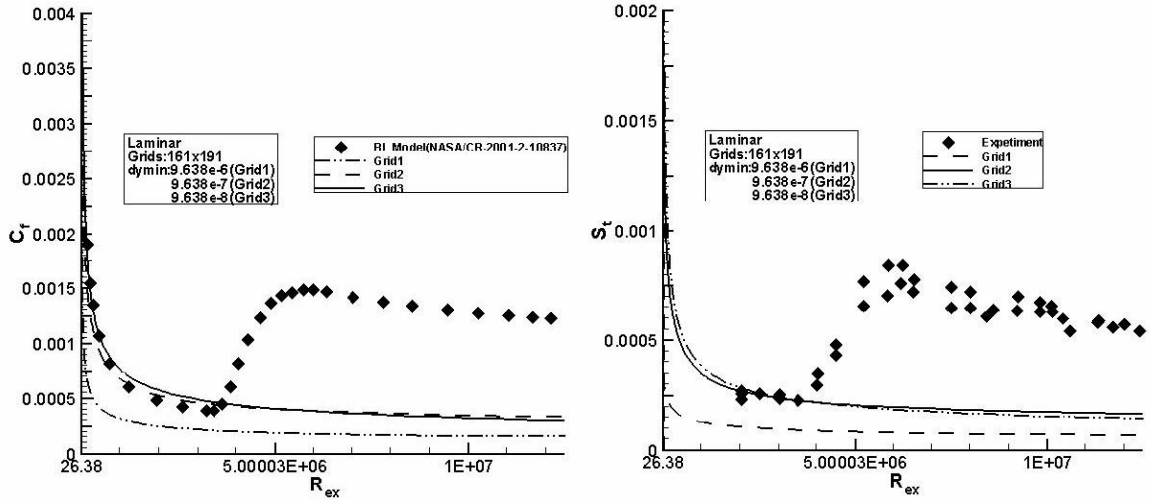

Fig. 12: Impact of wall friction coefficient and Stanton number for simulation of laminar flow caused by grid density

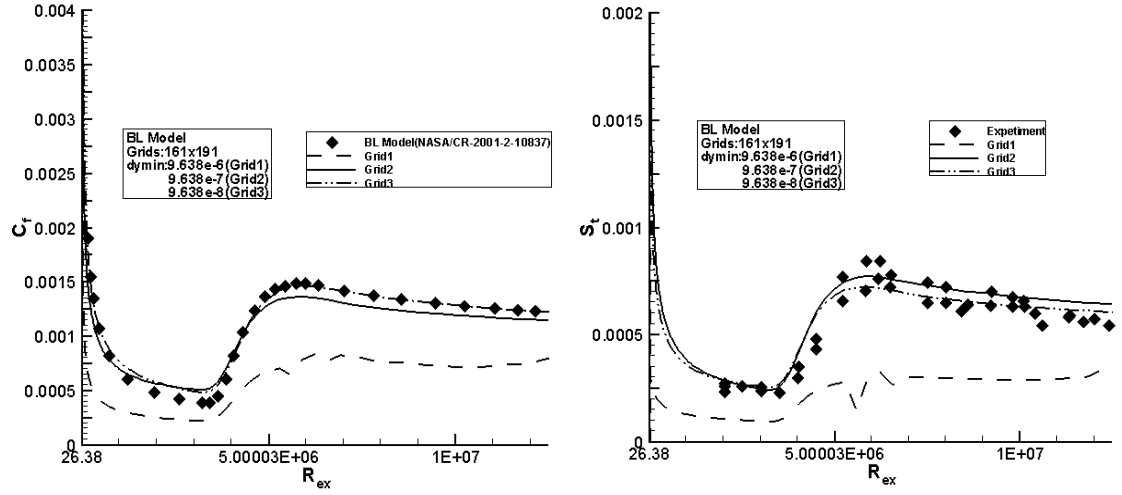

Fig. 13: Impact of wall friction coefficient and Stanton number for simulation of BL model caused by grid densit

Figure 13 shows the contrast between friction and the Stanton number of the BL model for the three grids. The Grid3 result was slightly better than that of Grid2 and the deviation between them was within 10%. The deviation of Grid1 was quite large with oscillation. The results of Grid3 and the calculation of Purtell (1992) were very close in the turbulence area.

Figure 14 shows the contrast between friction and the Stanton number of the SA model for the three grids. There existed a large difference only in the transition area for the results of Grid2 and Grid3. However, their errors and the error of the reference calculation remained within 10%. There occurred not only a large deviation for Grid1, but also certain oscillation in the laminar flow area. Figure 15 shows the contrast between friction and the Stanton number of the SST model for the three grids. There existed a difference only in the transition area for the results of Grid2 and Grid3. Both their errors were within 10%. The deviation of Grid1 was very large.

From the three grids, the contrast between friction and the Stanton number calculated by laminar flow and the three turbulence models were determined. To simulate more accurately the flow of the boundary layer and obtain proper surface friction and heat flow, the grid near the wall must be encrypted to an appropriate extent. The present study showed that a grid Reynolds number of 20 at the first grid layer was reasonable.

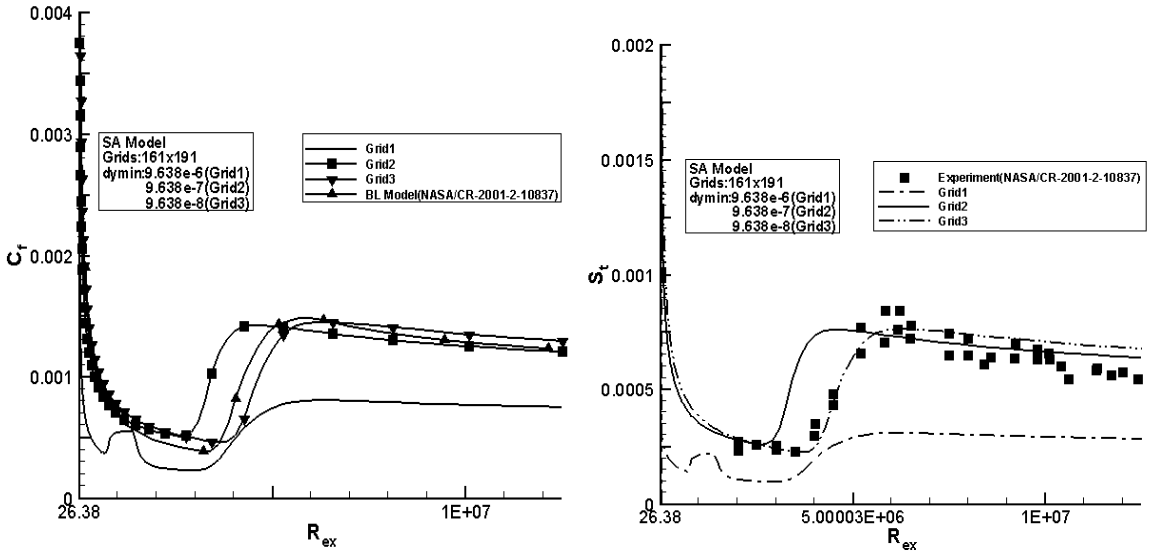

Fig. 14: Impact of wall friction coefficient and Stanton number for simulation of SA model caused by grid density

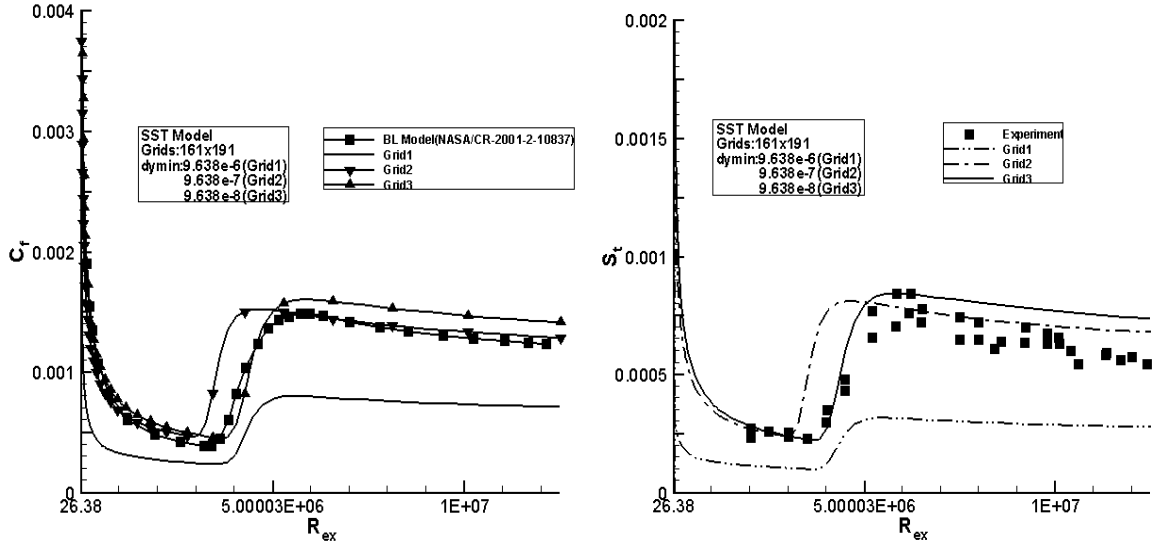

Fig. 15: Impact of wall friction coefficient and Stanton number for simulation of SST model caused by grid density

Table 2: Convergence process for three grid types

Grid	Laminar	BL model	SA model	SST model
Grid1	20 000	22 000	22 000	24 000
Grid2	24 000	24 000	28 000	28 000
Grid3	40 000	45 000	50 000	60 000

The approximate process for the calculated convergence of the three grids is shown in Table 2 The convergence process of Grid3 increased by twice that of Grid1 because of the greatly increased calculation time. This increase was caused by the grid encryption of the first grid layer under the same case of grid points.

Completing all the calculations by selecting Grid2 was a correct move, because Grid2 increased the calculation rate to nearly two-fold with an error of 10%. Therefore, the spacing of the first grid layer of the wall must be fully considered and reasonably resolved to improve calculation accuracy and computing time for practical engineering applications.

Isothermal two-dimensional wall corner: When an aircraft is flying at a high speed, the flow field of its controlling wing in the tail near the leading edge will cause such a complex flow phenomenon. Consequently, the shock wave and the turbulence boundary layer will interfere with each other. To numerically simulate this phenomenon, a simplified model is usually used. In this simple model, a two-dimensional compressible corner flow is employed to simulate the flow field of the controlling wing near the leading edge.

Flow condition: $M_\infty = 9.22$, $T_\infty = 64.5K$, and $R_{e\infty} = 4.73 \times 10^7(1/m)$

Body surface as isothermal wall: $T_W = 295\ K$

The calculation method involved using AUSMPW+ flux as the splitting method, min_3U as the interpolation limiter, discrete grid as the five-point template, original variable NND as the implicit scheme, Reynolds-average NS equation as the governing equation, finite volume as the discretization method and LU decomposition technique as the discrete equation.

Figure 16 shows the flow line near the corner. The result of the laminar flow exhibited a complex separated zone similar with a two-dimensional compression corner in the front corner. No separated zone in the flow field of the turbulence model simulation was observed.

Figure 17 shows the density line near the corner. On the laminar flow, the density distribution became very complex due to the existence of the separation zone in the corner. However, the density distribution of the turbulence model simulation was more regular because there was no separation zone.

Figure 18 shows the pressure line near the corner. The results of the laminar flow had a series of compression waves within long areas before the corner due to the existence of the separation zone in the corner. A shock position formed after the separation bubble was observed later in the two turbulence models. The results of the two turbulence models only had subtle differences.

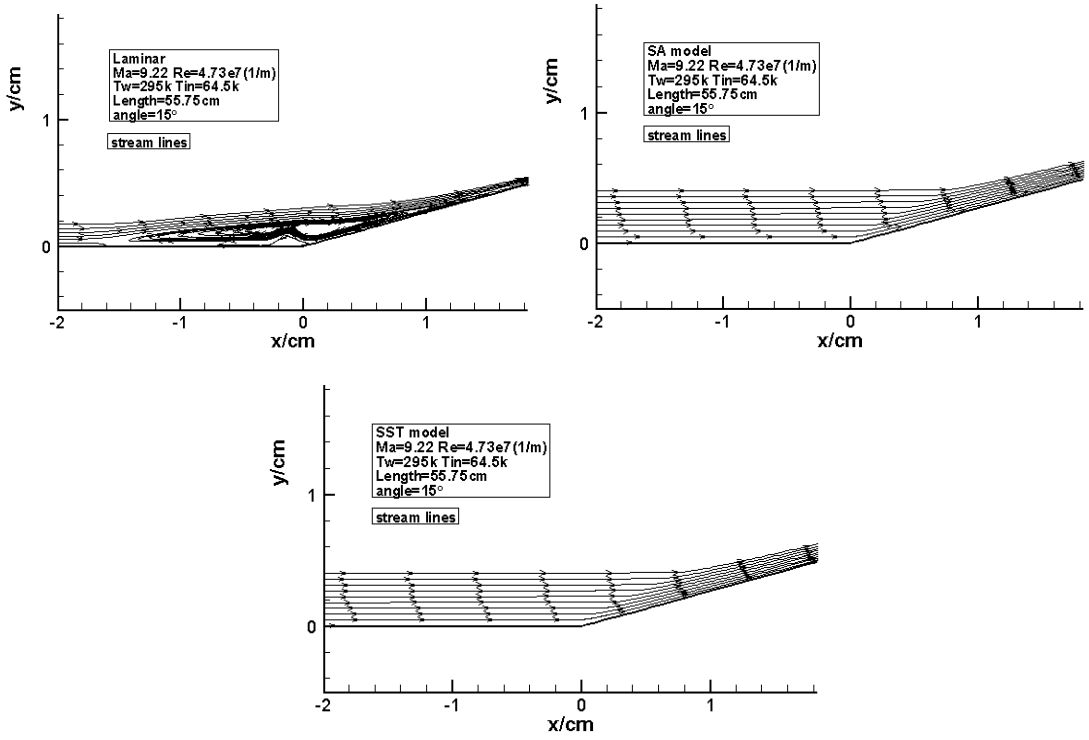

Fig. 16: Flow line near corner for simulation of laminar, SA model and SST model

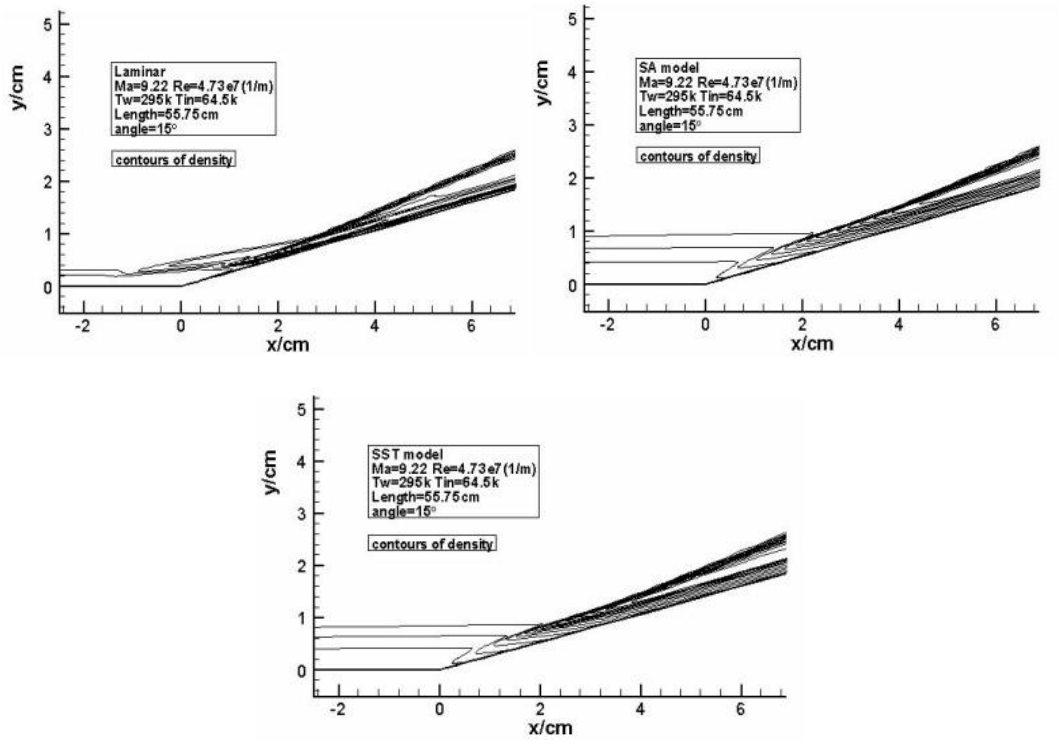

Fig. 17: Density line near corner for simulation of laminar, SA model and SST model

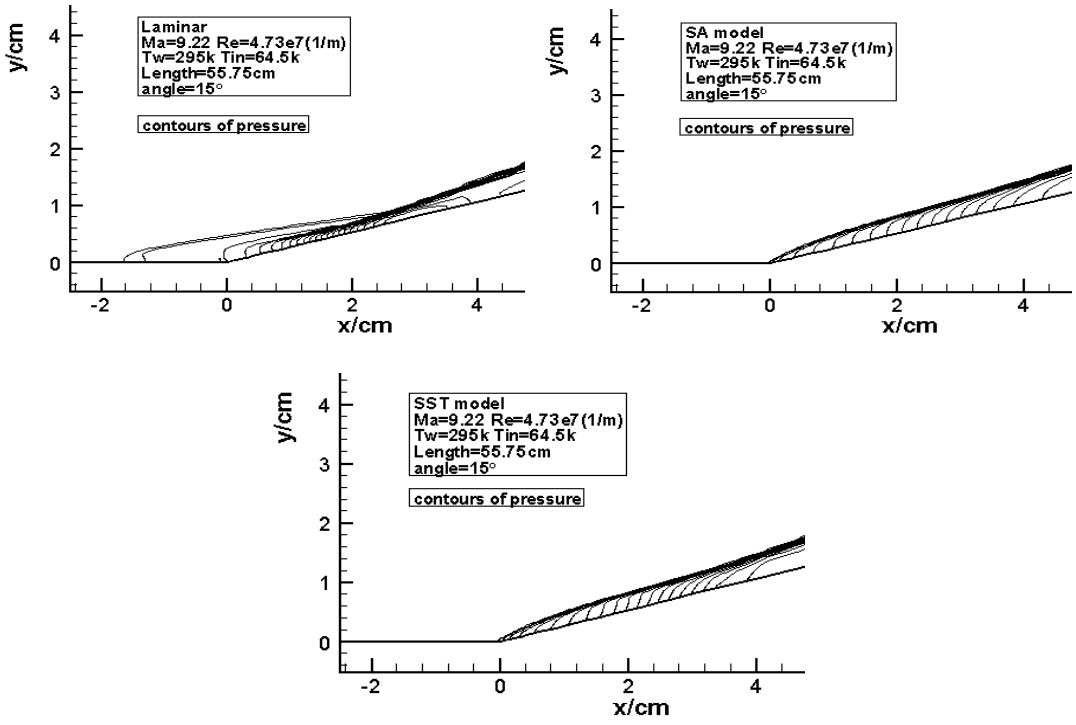

Fig. 18: Pressure line near corner for simulation of laminar, SA model and SST model

Figure 19 shows the calculation of the wall heat flow. The experimental data in the Figure came from reference (Suzen and Hoffmann, 1999). The symbol "SST model (ref)" represented the calculation given by reference (Purtell, 1992). The results of the two turbulence models were consistent. The position of the heat flow peak simulated by the two turbulence models was only slightly different from the experimental

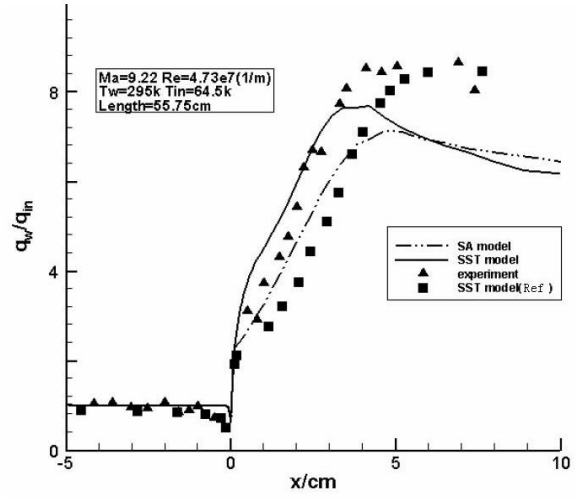

Fig. 19: Comparison of wall heat flow

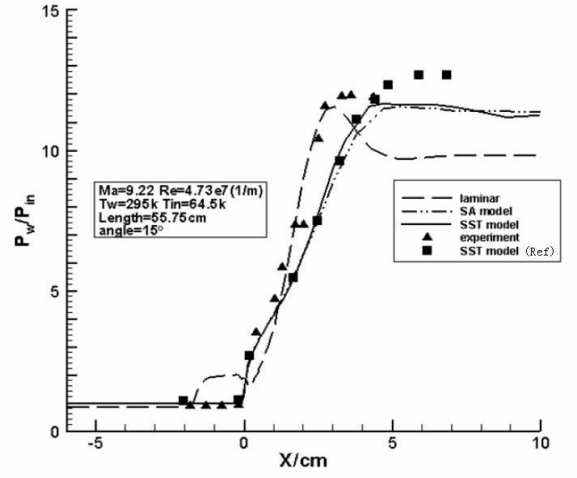

Fig. 20: Comparison of wall pressure distribution and reference result for different turbulence models

position. However, the peak, the curve trend after the peak and the experimental result had greater differences.

Figure 20 shows the comparison curve of the wall pressure distribution. The pressure distribution and the experimental result significantly differed from the result of the laminar flow due to the separation zone. However, the results of the two turbulence models and the experimental result were close. The curve trend and peak were consistent with the experimental result.

CONCLUSION

A numerical simulation for a hypersonic flat plate and two-dimensional corner turbulence flow was performed using a self-developed hypersonic CFD software platform. The following conclusions are drawn:

- The hypersonic Computational Fluid Dynamics (CFD) software platform considered the turbulence effect using the turbulence model. This model can significantly improve the prediction result. The agreement between the simulation of the flat boundary layer and the qualitative experimental result was verified.
- By choosing appropriate calculation models and methods as well as studying grid convergence, the hypersonic CFD software platform can accurately simulate the flow of a flat turbulence boundary layer. This finding indicated that the flow of a flat turbulence boundary layer was confirmed.

In the turbulence model with the same initiation but different flow fields, the convergence process of friction and the Stanton number of the hypersonic flat plate showed was revealed. The turbulence effect on the BL model was responsive to the heat flow and friction. The SA and SST models both reflected the development process of turbulence. The turbulence effect of the SST model did not gradually emerge until the laminar flow simulation was sufficient. Moreover, the SA model did not exist on such obvious hysteresis. By comparing the friction and Stanton number of the hypersonic flat plate simulation for and the laminar flow under the three grids, the errors on the calculation results of Grid2 and Grid3 were small, but the error on Grid1 was large. By comparing the friction and Stanton number of the BL model for the three grids, the result of Grid3 was found to be slightly better than the result of Grid2. The deviation between them remained within 10%, but the result of Grid1 had a large deviation with oscillation. The friction and Stanton number of the SA model for the three grids were then comparing. There was a large difference only on the transition zone location between the results of Grid2 and Grid3. However, the error and calculation of reference between them remained within 10%. Grid1 not only had a large deviation, but also had certain oscillation on the laminar flow area. Finally, the friction and Stanton number of the SST model for the three grids were compared. There was a large difference only on the transition zone location between the results of Grid2 and Grid3, but the error between them remained within 10%. Grid1 also had a large deviation. The hypersonic flat-plate laminar flow was subsequently compared with the friction and Stanton number calculated from the three turbulence models for the three grids. The grids near the wall must be encrypted to an appropriate extent to simulate more accurately the boundary laminar flow as well as obtain proper surface friction and heat flow. The calculation in the present study showed that a Reynolds number of about 20 in the first grid layer were reasonable.

The simulation results of a hypersonic isothermal two-dimensional corner wall flow were consistent with the experiment results of different turbulence models. The position of the simulated heat flow peak and the experimental position had little difference. The peak, the curve trend after the peak and the experiment result had greater differences. The comparison between the curve of pressure distribution and the experiment result were significantly different. This difference is attributed to the existence of a separation zone on the laminar flow calculation. The calculation and experimental results of different turbulence models were close. The curve trend and peak were basically consistent with the experimental result.

ACKNOWLEDGMENT

This study was supported by the Northwestern Polytechnical University Basic Research Fund and the Chinese Aerospace Innovation and Technology Fund.

REFERENCES

Arthur, D.D., 2001. Evaluation of CFD turbulent heating prediction techniques and comparison with hypersonic experimental data. Technical Report NASA/CR-2001-210837.

Gao, X.C., 2005. Validations of hypersonic aerodynamic software. MS Thesis, Northwestern Polytechnical University., Xian, China.

Holden, M., 2002. Experimental Studies of Laminar Separated Flows Induced by Shock Wave/Boundary Layer and Shock/Shock Interaction in Hypersonic Flows for CFD Validation. AIAA 2000-0930, 2000.

Jean, M., K. Ajay and D. Christian, 1998. Hypersonic Experimental and Computational Capability, Improvement and Validation. (l'Hypersonique Experimentale Et de Calcul - Capacite, Ameliorafion Et Validation. Advisory Group for Aerospace Research and Development Neuilly-Sur-Seine, France, pp: 172.

Purtell, L.P., 1992. Turbulence in Complex Flows: A Selected Review. AIAA-1992-0435.

Suzen, Y.B. and K.A. Hoffmann, 1999. Application of Several Turbulence Models for High Speed Shear Layer Flows. AIAA-99-0933.

Yamamoto, Y., 2001. CFD Study and Validation Process of Hypersonic Aerodynamics for the Space Transport Systems Including HOPE-X. AIAA 2001-1854.